




Early Life Social Stress Causes Sex- and Region-Dependent Dopaminergic Changes that Are Prevented by Minocycline

Clarissa Catale¹ · Luisa Lo Iacono² · Alessandro Martini³ · Constantin Heil⁴ · Ezia Guatteo^{3,5} · Nicola Biagio Mercuri^{3,6} · Maria Teresa Viscomi^{7,8} · Daniela Palacios^{4,8,9} · Valeria Carola^{1,2} 

Received: 29 November 2021 / Accepted: 2 April 2022 / Published online: 18 April 2022
© The Author(s) 2022, corrected publication 2022

Abstract

Early life stress (ELS) is known to modify trajectories of brain dopaminergic development, but the mechanisms underlying have not been determined. ELS perturbs immune system and microglia reactivity, and inflammation and microglia influence dopaminergic transmission and development. Whether microglia mediate the effects of ELS on dopamine (DA) system development is still unknown. We explored the effects of repeated early social stress on development of the dopaminergic system in male and female mice through histological, electrophysiological, and transcriptomic analyses. Furthermore, we tested whether these effects could be mediated by ELS-induced altered microglia/immune activity through a pharmacological approach. We found that social stress in early life altered DA neurons morphology, reduced dopamine transporter (DAT) and tyrosine hydroxylase expression, and lowered DAT-mediated currents in the ventral tegmental area but not substantia nigra of male mice only. Notably, stress-induced DA alterations were prevented by minocycline, an inhibitor of microglia activation. Transcriptome analysis in the developing male ventral tegmental area revealed that ELS caused downregulation of dopaminergic transmission and alteration in hormonal and peptide signaling pathways. Results from this study offer new insight into the mechanisms of stress response and altered brain dopaminergic maturation after ELS, providing evidence of neuroimmune interaction, sex differences, and regional specificity.

Keywords Early life stress · Sex differences · Ventral tegmental area · Substantia nigra · Microglia · RNA sequencing

Introduction

Adverse childhood experiences can modify trajectories of brain development, leading to aberrant maturation that increases risk for psychopathologies and neurological

Daniela Palacios and Valeria Carola are equal senior author

✉ Valeria Carola
valeria.carola@uniroma1.it

¹ Division of Experimental Neuroscience, Neurobiology of Behavior Laboratory, IRCCS Santa Lucia Foundation, Rome, Italy

² Department of Dynamic and Clinical Psychology, and Health Studies, Sapienza University of Rome, Via degli Apuli 1, Rome, Italy

³ Division of Experimental Neuroscience, Experimental Neurology Laboratory, IRCCS Santa Lucia Foundation, Rome, Italy

⁴ Division of Experimental Neuroscience, Epigenetics and Signal Transduction Laboratory, IRCCS Santa Lucia Foundation, Rome, Italy

⁵ Department of Motor Science and Wellness, University of Naples Parthenope, Naples, Italy

⁶ Department of Systems Medicine, Università Degli Studi Di Roma Tor Vergata, Rome, Italy

⁷ Department of Life Science and Public Health, Section of Histology and Embryology, Università Cattolica Del S. Cuore, Rome, Italy

⁸ IRCCS Fondazione Policlinico Universitario A. Gemelli, Rome, Italy

⁹ Department of Life Science and Public Health, Section of Biology, Università Cattolica Del S. Cuore, Rome, Italy

disorders [1, 2]. Among the most consistent changes observed in maltreated individuals are alterations in structure and function of reward-associated brain regions, specifically the mesocorticolimbic and nigrostriatal dopaminergic pathways, which originate in the ventral tegmental area (VTA) and substantia nigra (SN), respectively [1, 3–5]. Such dopaminergic alterations have been associated with all kinds of mental disorders and are thought to be etiological factors for certain psychopathological outcomes, especially substance use disorders [6–9]. In this context, human research is still mostly correlational because of the difficulty in performing studies that reliably draw causal inference, especially in children [10]. Animal studies have demonstrated that early life stress (ELS) induces changes in the dopamine (DA) system in terms of excitability, receptor number, receptor sensitivity, DA reuptake, and metabolism as a function of the age of exposure to the stress, the life stage at which the stress effects are measured, and the type and duration of adversity [9, 11]. Moreover, these changes are paralleled by variations in behavioral domains that may predispose to psychiatric outcomes [4, 6, 9, 12–14]. Although preclinical research has contributed tremendously to this topic, knowledge about the biological mechanisms by which ELS alters development of the DA system is still scarce.

One of the actors involved in guiding DA system development is the brain's resident immune compartment, namely microglia. Studies have established that during brain development, microglia contribute directly to the correct maturation of the DA system and DA-dependent behaviors, by regulating outgrowth of dopaminergic axons in the mouse embryonic forebrain [15] and pruning the levels of DA receptors in adolescent male rats [16]. Other studies have shown that ELS can trigger microglia “activation” in rodent models and an enduring systemic inflammatory phenotype in both humans and animals [17, 18]. Based on these findings, it has been proposed that ELS interferes with microglia and immune system developmental trajectories, resulting in aberrant neural maturation and brain function and increased risk for neurodevelopmental, neuropsychiatric, and neurological disorders [17–20]. However, whether and how ELS modifies the interaction between microglia and DA system during development is still unknown.

Recently, we reported that exposure to a threatening social environment (social stress, SS) in the juvenile period in mice brings about microglia activation and aberrant DA-induced self-inhibitory responses of DA neurons in the developing VTA, and sensitivity towards the effects of cocaine later in life [21, 22]. Treatment with minocycline, an inhibitor of microglia activation, or GW2580, a selective inhibitor of macroglia/macrophage functionality, during SS normalizes microglia and dopamine sensitivity in the VTA and prevents the development of cocaine susceptibility [22].

Following these results, here we used the SS model [20–25] to evaluate the impact of ELS on markers of dopaminergic functionality and development in the VTA and SN of male and female mice. Furthermore, we tested whether microglia were implicated in the emergence of SS-induced dopaminergic changes by using minocycline. Finally, a transcriptome analysis in control and SS pups VTA was performed to evaluate biological pathways involved in ELS-induced dopaminergic changes.

Materials and Methods

Animals and Breedings

Seven-week-old CD-1 (CD1) male and DBA2/J @Ico (DBA) male and female mice were purchased from Charles River Laboratories (Calco, Italy). DBA male and female mice were mated at 12 weeks of age, with max 3 females and 1 male per cage. Pregnant mothers were single housed around gestation day 16. Each male was used for producing max 2 litters, and each mother (*primipara*) was used for producing only one litter to rule out the effects of changes in maternal behavior across pregnancies. Mice were kept at constant temperature (21 ± 1 °C) and humidity (55 ± 5 percent). Food and water were provided ad libitum, and mice were housed on a 12:12 light:dark cycle with lights on at 07.00 a.m. All experiments were carried out in accordance with Italian national law (DL 26/2014) on the use of animals for research based on the European Communities Council Directive (2010/63/UE) and comply with the ARRIVE guidelines. Experiments were approved by the ethics committee of the Italian Ministry of Health (license/approval IDs: #42/2015-PR; #677/2019-PR) and by local Ethical Committee of the Santa Lucia Foundation. All efforts were made to minimize the number of animals used and their suffering.

Early Life Social Stress

The SS model is a validated model of early life social stress [21] established in our laboratory [20–25]. As previously demonstrated, the SS paradigm does not alter overall maternal behavior towards the pups [21]. DBA litters with an average number of 5 pups (min 4, max 6 pups) were included in the study. Mouse pup litters were randomly (blind to litter features) assigned to unhandled control (CTR) or SS group at postnatal day (PD) 14. In each litter, max 2 mice/sex/group were used for experiments shown here. In the CTR group, mothers and offspring were left undisturbed until sacrifice (PD22). In the SS group, each pup was housed in a cage with a resident adult CD1 male mouse for 30 min per day from PD 14 to 21 (Fig. 1A) [21]. To avoid physical attacks to the pups, CD1 males were gonadectomized

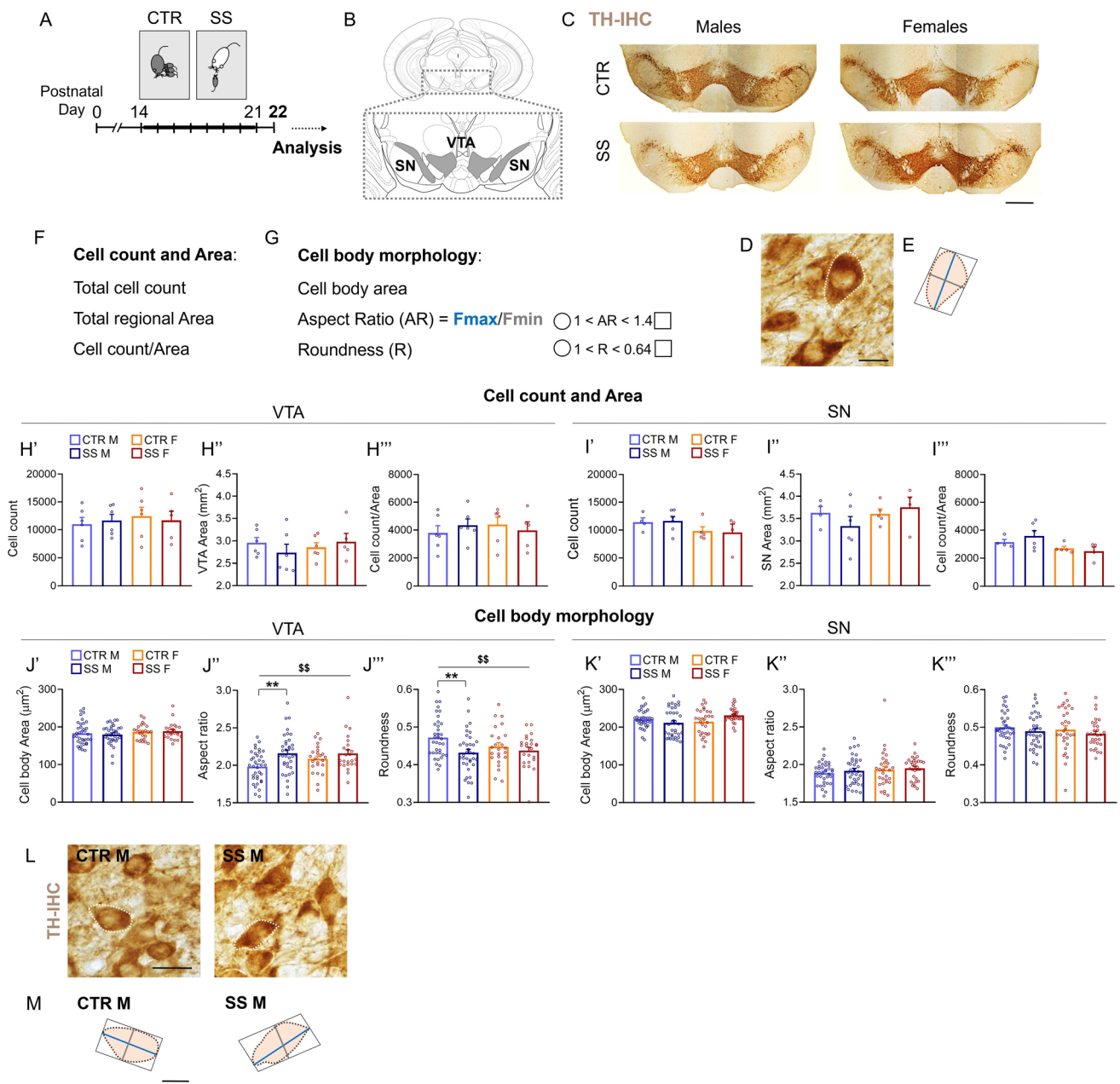


Fig. 1 Early life social stress changes dopaminergic neurons morphology in the VTA but not SN of male mice only. **A** Social stress (SS) protocol was applied from postnatal days (PDs) 14 to 21 and animals were sacrificed at PD22. **B** Schematic of coronal ventral midbrain section containing the Ventral Tegmental Area (VTA) and Substantia Nigra (SN) (Bregma \approx -3.52 mm, based on 27). Analyses were performed on the parabrachial pigmented and paranigral nuclei of the VTA and the pars compacta of the SN. **C, D** Representative images showing dopaminergic neurons in the VTA and SN at **C** lower and **D** higher magnification as revealed by tyrosine hydroxylase (TH) immunohistochemistry (IHC). **E** Representative reconstruction of a TH+neuron with maximum (Fmax, blue) and minimum (Fmin, gray) diameter (or feret) of the cell. **F, G** Parameters analyzed. **G** Aspect ratio (AR) is the ratio of Fmax and Fmin. A circle has an AR and R of 1 and a square has an AR of 1.4 and a R of 0.64. **H'–H'''**, **I'–I'''** No significant difference in **H'**, **I'** total TH+cell count, **H''**, **I''** TH+area, and **H'''**, **I'''** cell count/area was detected between SS

and CTR mice in both regions and sexes. **J'–J'''** Significant differences in aspect ratio and roundness but not cell body area, were found between SS and CTR mice in the VTA (**J'–J'''**; MANOVA, univariate group effect: $P < 0.01$). Specifically, SS significantly altered the shape of DA neurons somata in the VTA of male but not female mice, increasing the aspect ratio and decreasing the roundness (**J'**, **J'''**; Tukey HSD test: $P < 0.001$). Such differences were not detected in (**K'–K'''**) male or female SN. Representative images (L) and reconstruction (M) of male VTA TH+neurons in CTR and SS mice. Dopaminergic neurons in SS mice appear more squared, with a longer maximum diameter (blue) and a shorter minimum diameter (gray). **H'–H'''** $N = 5–6$ animals/group/sex. Dots in the graphs represent average value for each animal. **J'–K'''** $N = 4–6$ animals/group/sex; 6 hemisections/animal. Dots in the graphs represent average value for each hemisection. Univariate group effect: $\$ \$ P < 0.01$; Tukey HSD test: $**P < 0.01$. Data are presented as mean \pm s.e.m. Scale bars = (C) 500 μ m; (D, M) 10 μ m, (L) 20 μ m

and single housed 1 month before the beginning of early life stress procedures. Limited cage cleaning was performed in the offspring cage from birth to weaning to avoid handling of the pups. DBA mice were sacrificed at PD22 for experiments.

Minocycline Treatment

For minocycline experiments, CTR and SS pups received daily intraperitoneal (i.p.) injection of minocycline hydrochloride (50 mg/kg; Sigma-Aldrich, #M9511) [22, 26] dissolved in sterile saline solution (2.5 mg/ml) from PD14 to PD21. For SS mice, injection was performed 1 h prior to the stress procedure [22].

Immunohistochemistry

At PD22, 4–6 mice per sex per group were anesthetized with Rompun (20 mg/ml, 0.5 ml/kg, i.p., Bayer) and Zoletil (100 mg/ml, 0.5 ml/kg, Virbac) and perfused transcardially with 20-ml saline followed by 20 ml of 4% paraformaldehyde (PFA) in phosphate buffer (PB) (0.1 M, pH 7.4). Brains were post fixed in 4% PFA overnight at 4 °C and then immersed in a 30% sucrose-PB solution until sinking. Afterwards, brains were cut into 30- μ m-thick coronal sections using a freezing microtome.

For stereological and morphological analyses of dopaminergic neurons, every second slice approximately between – 3.08 and – 3.80 mm from Bregma (based on [27]) containing the VTA and SN was selected, for a total of 8 sections. Sections were treated for 5 min with 0.3% H₂O₂ to block endogenous peroxidase and then incubated for 48 h at 4 °C with rabbit anti-tyrosine hydroxylase (TH) antibody (1:700; #sc-25269, Santa Cruz Biotechnologies) for detection of dopaminergic neurons. TH is the rate-limiting enzyme in the synthesis of dopamine and marks dopamine neurons in the VTA and SN. Then, sections were incubated for 2 h with a biotinylated donkey anti-rabbit antibody (1:200, #BA-1000, Vector Laboratories), followed by 2 h in an ExtrAvidin solution (1:1000; #E2886, Sigma-Aldrich) at room temperature. As chromogen, 3,3'-diaminobenzidine 0.05% (#D5637, Sigma-Aldrich) was used. Primary and secondary antibody solutions as well as ExtrAvidin solutions were prepared in PB and 0.3% Triton X-100. Each incubation step was followed by three 5 min rinses in PB. The specificity of immunohistochemical labeling was evaluated based on established guidelines on TH+ staining in the midbrain [28, 29]. Sections from all experimental groups were processed together to allow quantitative comparisons. Finally, sections were mounted on chrome-alum-coated slides, air-dried, dehydrated, and coverslipped.

For immunofluorescence staining, a total of 4–6 regularly spaced sections of VTA and SN (between – 3.08 and

– 3.80 mm from Bregma, based on [27]) were selected for each animal. Sections were incubated for 48 h at 4 °C with the primary antibodies including rabbit anti-TH (1:700; #sc-25269, Santa Cruz Biotechnologies) and rat anti-DAT (1:200; #sc-32259, Santa Cruz Biotechnologies), followed by 2-h incubation of secondary antibodies including Alexa Fluor 555 conjugated donkey anti-rabbit (#A-31572, 1:200; ThermoFisher Scientific) and Alexa Fluor 488 conjugated donkey anti-rat (#A-21208) at room temperature. Primary and secondary antibody solutions were prepared in PB 0.3% Triton X-100, and each incubation step was followed by three 5-min rinses in PB. To avoid staining variability, sections from all groups were concomitantly incubated with the same cocktail of primary and secondary antibodies. The specificity of immunohistochemical labeling was confirmed by the omission of primary antibody and the use of normal serum instead (negative controls, Supplementary file1 Fig. 2). Sections were rinsed, DAPI-counterstained, mounted using an anti-fade medium (Fluoromount; Sigma-Aldrich), and coverslipped.

Stereological and Morphological Analyses of Dopaminergic Neurons

Sections processed for TH immunohistochemistry were used for obtaining unbiased estimates of total number and morphology of TH+ neurons, and total surface area of the VTA and SN. The boundaries of these areas were defined by TH staining, according to published guidelines [27]. In the VTA, analysis was restricted to the parabrachial pigmented nucleus (PBP) and paranigral nucleus (PN) subareas, where TH+ neurons are known to express classical dopaminergic markers such as vesicular monoamine transporter 2, dopamine transporter (DAT), and the dopamine receptor D2 (DRD2), and project to regions implicated in reward processing, such as the nucleus accumbens [28, 29]. In the SN, analysis was performed in the pars compacta, where the majority of cell bodies are TH+. We applied an optical fractionator stereological design (bilateral count) using the Stereo Investigator System (MicroBrightField Europe e.K.) as previously described [30]. Data collection was done blind to the experimental group of each animal.

Neuronal morphology analysis on sections processed for TH immunohistochemistry was performed using an optical microscope (DMLB, Leica) equipped with a motorized stage and a camera connected to the Neurolucida 7.5 software (MicroBrightField) [31, 32]. Three sections containing the VTA/SN were selected, and 8 random cells in each hemisphere (6 hemisections including 3 right and 3 left VTAs and SNs) were included in the analysis, for a total of 48 cells per animal per structure. The VTA and SN were detected using the 5 \times objective, and neuronal cells were analyzed with a 100 \times oil-immersion objective. Cell bodies were

manually outlined, and a set of parameters from the “Contour Measurement” analysis of the NeuroLucida Software (<https://www.mfbioscience.com/help/si11/Content/Contours/contourmeasure.htm>) were collected to evaluate somatic shape based on literature [31, 33]: cell body area, aspect ratio, and roundness. Aspect ratio is the ratio between feret maximum and feret minimum, and feret maximum and minimum are defined as “the largest and smallest dimensions of the contour as if a caliper was used to measure across the contour” (from NeuroLucida User Guide, Fig. 1E). Only TH+ neurons that displayed intact soma and round nuclei were included. For final figures, images were acquired with the 5× or 100× oil-immersion objectives, exported in TIFF format, and adjusted for contrast and brightness equally across the entire image and across groups. Representative images of ventral midbrain TH+ areas (Fig. 1C) were reconstructed from single hemisphere images acquired with the 5× objective.

Quantitative Analysis of Fluorescence Images

Sections were examined through a confocal laser scanning microscope (Zeiss CLSM800). Acquisitions of one left or right hemisphere per section (hemisections) were performed by using a 20×/0.50 objective (Plan-Apochromat, Zeiss) so that all samples within each experiment were captured using consistent settings for laser power and detection gain. Images were acquired at 1024×1024-pixel resolution (image size 638.9 μm per side) and 8-bit depth and exported in carl zeiss image format (.czi). PBP and PN subareas of the VTA, and distinction between VTA and SN were identified with the aid of an atlas [27]. Analyses were performed by using the ImageJ software [34] on .czi acquisitions. No changes in brightness and contrast were applied for the analyses. Background was removed by placing a small region of interest (ROI) (15 μm per side) on an area with no specific signal and applying the “BG (background) subtraction from ROI” plugin. Subsequently, TH and DAT signals were quantified by measuring fluorescence intensity as mean gray value within a ROI positioned on the PBP/PN (300 μm per side) and SN pars compacta (200 μm per side) in 4 (TH) or 6 (DAT) regularly spaced sections per animal. All analyses were performed blinded to the mouse experimental group. For final figures, images were acquired through the 20× or oil immersion 63× (insets) objectives, exported in TIFF format and contrast and brightness were adjusted equally across the entire image and across groups.

Electrophysiological Experiment

Preparation of midbrain slices ($N=3$ mice/group) was performed as described previously [22, 35]. Briefly, mice were anesthetized with halothane and decapitated. Horizontal

midbrain slices (thickness 250 μm) containing the VTA were cut within artificial cerebrospinal fluid (aCSF, 22) at 6–8 °C and left to recover in a holding chamber (32–33 °C) for 30 min prior to usage. A single slice was placed into a recording chamber (0.6 mL) of an upright microscope (BX51WI; Olympus) and continuously perfused with aCSF (33 °C) saturated with a 95% O₂/5% CO₂ gas mixture at a constant flow rate (2.5 mL/min). Slices were visualized with a microscope’s in-built CCD camera (Photometrics Evolve). Referring to the mouse practical map of DA neuron location in distinct VTA subregions previously reported by our group [36] and others [37], we performed electrophysiological recordings from DA neurons located in the lateral and intermediate VTA. As opposed to medial VTA, DA neurons belonging to these subregions produce similar responses to exogenous dopamine application [36–38]. Cell-attached and whole-cell patch clamp recordings were conducted according to Lo Iacono et al. [22]. Only DA-sensitive neurons simultaneously meeting the following criteria were included: slow and regular pacemaker firing (0.5–4 Hz) in the cell-attached configuration, action potential duration ≥ 1.2 ms in the cell-attached configuration and I_h amplitude ≥ -50 pA at -120 mV in whole-cell configuration. Non-firing cells in the cell-attached configuration were abandoned.

DAT-mediated inward currents were elicited by bath application of DA in the presence of the DRD2 antagonist sulpiride, to prevent activation of large DRD2-GIRK2 inhibitory outward currents. Excitatory DAT-current is generated by uptake of DA (against concentration gradient) co-transported with 2 Na⁺ and 1 Cl⁻ along their ionic gradients [39–42], and reverts polarity at membrane potential more positive (-47 mV) than holding potential (-60 mV), thus causing a net excitation/inward current in DA neurons [43–45]. DA (30 μM; H8502, Sigma-Aldrich) and L-sulpiride (5 μM; Sigma-Aldrich) were bath applied via a three-way tap syringe containing the drug at final concentration, dissolved in warm aCSF, saturated with a 95% O₂/5% CO₂. To unmask the DA-induced inward current mediated by DAT [46], sulpiride was applied 5 min prior to DA application. Stock solutions were freshly prepared on the day of the experiment. Drugs were applied only once per slice, in order to avoid possible receptor desensitization and/or cross-interactions between cells, and within 10 min after the establishment of the whole-cell configuration. DA application lasted until the DA-induced inward current reached a plateau in the whole-cell configuration. All recordings were performed blinded to the experimental group.

RNA Purification from VTA Punches

Male pups were decapitated at PD22 ($N=4$ /group) and brains were dissected, deprived of cerebellum and pons-medulla, and stored at -80 °C. Punches of VTA were

obtained from coronal brain slices no thicker than 300 μm according to Ventura et al. [47] and with the aid of a mouse brain atlas [27]. A stainless steel tube of 0.5 mm internal diameter was used to punch left and right VTAs, which were then collected in the same tube and stored in liquid nitrogen until further processing. RNA was then isolated using Total RNA purification Kit (Norgen Biotek). RNA from individual VTA samples (about 200 ng each) were quantified and quality tested by Agilent 2100 Bioanalyzer RNA assay (Agilent technologies). Only RNA samples with RIN value > 7.0 were included in the study.

RNA Library Preparation and Sequencing

mRNA sequencing was performed at IGA technology service (Udine, Italy). Universal Plus mRNA-Seq kit (Tecan Genomics, Redwood City, CA) has been used for library preparation following the manufacturer's instructions. Final libraries were checked with both Qubit 2.0 Fluorometer (Invitrogen, Carlsbad, CA) and Agilent Bioanalyzer DNA assay or Caliper (PerkinElmer, Waltham, MA). Libraries were then sequenced on single-end 75 bp mode on NextSeq 500 (Illumina, San Diego, CA). On average 30 million reads were produced per sample.

Bioinformatic Analyses of RNA-seq Data

Read quality was asserted through FastQC, and quality/adaptor trimming was carried out using Cutadapt. Single end reads were aligned to mouse reference mm10 using STAR aligner. Subsequently, reads were counted for genes using htseq-count (features from Ensemble gtf file, ftp://ftp.ensembl.org/pub/release-102/gtf/mus_musculus/). Read counts were then input into DESeq2 in R, and differential expression analysis was conducted with default options [48]. Genes were considered differentially expressed if the adjusted p -value was less than 0.05. Subsequent to scaling of raw read counts and execution of differential expression analysis, read counts were transformed by DESeq2's variance stabilizing transformation (VST), in order to stabilize read count variance as a function of total reads number. Transformed gene expression for genes with adjusted p -value less than 0.05 was standardized and plotted in the heatmap. Rows and columns underwent hierarchical clustering, considering Euclidean distance as distance metric. Heatmap plot was performed using the pheatmap R-package. Gene ontology analyses and gene networks were obtained by Ingenuity pathway analysis (QIAGEN Redwood City, www.qiagen.com/ingenuity). Over-representation analysis was carried out using the R packages DOSE and ReactomePA [49, 50]. The significance of enrichment is determined through application of the hypergeometric test.

RNA-seq Data Availability

RNA-Seq data are available through NCBI's Gene Expression Omnibus (GEO) repository, under accession number GSE199136.

Statistics

All data were first checked for normality by graphical inspection of the residuals' distribution and for homogeneity of variances with the Levene's test. VTA and SN were analyzed separately. Analysis of the main effects of group and sex, and interactions between these variables on immunohistochemical data was performed with two-way analysis of variance (ANOVA). In case of main factor or interaction significance ($P < 0.05$), ANOVA was followed by planned post hoc comparisons (Tukey HSD test) and nested (hierarchical) one-way ANOVA. Nested ANOVA was performed to take into account variability within samples (between observations from the same animal) as well as variability within and between groups [51]. In nested ANOVA, the group (CTR vs SS) was considered as fixed factor, and the animals and observations (cells/sections) were considered as random factors, and sample sizes (N of animals) in the groups and number of observations per sample were kept equal. Electrophysiological data were subjected to parametric Student's t -test (t -test). Minocycline experiments were analyzed by two-way ANOVA, considering group (stress) and treatment (minocycline) as main factors. For all tests, significance was set at $P < 0.05$. All data are expressed as mean \pm standard error of the mean (s.e.m.). Statistica software Version 12.0 (StatSoft, Tulsa, OK, USA) was used to perform the statistical analyses.

Results

Early Life Social Stress Does Not Alter the Number of Dopaminergic Neurons nor the Total Area of the VTA and SN

Since it has been demonstrated that dopaminergic neurons undergo a wave of physiological death/apoptosis at PD14 [52], and that social stress either in the first two postnatal weeks or in adulthood can affect the number of DA neurons [31, 53], we tested whether our model of social stress (SS) applied during the third postnatal week could alter the number of DA neurons and the total area of the VTA (PBP and PN) and SN (pars compacta) in male and female PD22 pups (Fig. 1A–C, F). DA neurons were identified by means of tyrosine hydroxylase (TH) immunostaining (Fig. 1C). Multivariate two-way ANOVA (MANOVA) of stereological measures (number of TH+ neurons, total area of

the TH+ region, and number of cells/area) in the VTA failed to reveal any significant group (CTR vs SS; $\lambda = 0.99$, $F_{3,17} = 0.07$, $P = 0.98$), sex (M vs F; $\lambda = 0.95$, $F_{3,17} = 0.31$, $P = 0.82$), or group*sex ($\lambda = 0.93$, $F_{3,17} = 0.44$, $P = 0.73$) effect (Fig. 1H'-H'''); males: $N = 6$ animals/group, females: $N = 5-6$ /group). Similar results were obtained for the SN (Fig. 1I'-I'''), MANOVA, group effect: $\lambda = 0.92$, $F_{3,13} = 0.36$, $P = 0.78$; sex effect: $\lambda = 0.68$, $F_{3,13} = 2.03$, $P = 0.16$; group*sex effect: $\lambda = 0.87$, $F_{3,13} = 0.64$, $P = 0.60$; males: $N = 4-6$ animals/group, females: $N = 4-5$ /group). These results indicate that male and female CTR and SS mice display similar DA neurons number and VTA/SN total area.

SS Alters the Morphology of Dopaminergic Neurons in the VTA but Not SN of Male Mice Only

Chronic adult social stress can reduce the size of DA neurons [53], and soma size and morphology of DA neurons have been associated with altered functionality of these cells and aberrant behaviors [12, 54]. Therefore, we characterized morphological profiles of the soma of DA neurons in SS and CTR mice by evaluating cell body area and other shape indices, including the aspect ratio and roundness [33] (Fig. 1D, E, G). MANOVA of somatic shape indices in the VTA showed a significant main effect of the group ($\lambda = 0.93$, $F_{3,114} = 2.90$; $P = 0.036$), but no significant effect of sex ($\lambda = 0.97$, $F_{3,114} = 1.30$; $P = 0.29$) or group*sex interaction ($\lambda = 0.97$, $F_{3,114} = 1.30$; $P = 0.27$; males: $N = 6$ animals/group, 6 hemisections/animal; females: $N = 4$ animals/group; 6 hemisections/animal). Univariate results indicated a significant group effect only on aspect ratio ($F_{1,116} = 8.84$; $P = 0.0036$) and roundness ($F_{1,116} = 6.88$; $P = 0.0099$), but not on cell body area (Fig. 1J'-J'''). Post hoc comparison revealed significant differences between male CTR and SS mice (aspect ratio: $P = 0.0060$; roundness: $P = 0.0071$), but not between female CTR and SS animals (Fig. 1J'',J'''). The difference in somatic shape between male CTR and SS VTA was further confirmed by nested ANOVA (cell(animal(group)): aspect ratio $F_{1,564} = 16.78$, $P < 0.001$; roundness $F_{1,564} = 20.43$, $P < 0.001$; $N = 6$ animals/group, 48 cells/animal), demonstrating that SS male DA neurons present an altered, elongated shape, with reduced short axis and augmented long axis, resulting in increased aspect ratio and decreased roundness compared to CTR (Fig. 1L, M).

This effect was restricted to the VTA, as no significant main or interaction effect was detected in the SN (Fig. 1K'-K'''), MANOVA group effect: $\lambda = 0.97$, $F_{3,126} = 1.10$, $P = 0.35$; sex effect: $\lambda = 0.96$, $F_{3,126} = 1.70$, $P = 0.16$; group*sex effect: $\lambda = 0.95$, $F_{3,126} = 2.30$, $P = 0.077$; males: $N = 6$ animals/group, 6 hemisections/animal; females: $N = 5$ animals/group; 6 hemisections/animal).

SS Reduces Expression of the Dopamine Transporter and Tyrosine Hydroxylase Proteins in the Developing VTA but Not SN of Male Mice Only

We performed immunofluorescence staining and confocal imaging to assess distribution and expression of dopamine transporter (DAT) and tyrosine hydroxylase (TH) proteins (Fig. 2A, B), which are canonical markers of dopaminergic neurons [29, 55] and have shown to be modulated by adult and early life social stress [11]. Two-way ANOVA on quantitative measurements of DAT intensity showed significant group*sex interaction effect in the VTA ($F_{1,116} = 5.07$, $P = 0.026$) but not in the SN ($F_{1,116} = 1.40$, $P = 0.24$), and no main effect of group or sex in either region (Fig. 2C, E; $N = 5$ animals/group/sex, 6 sections/animal). Similar results were obtained for TH intensity (Fig. 2D, F, Two-way ANOVA, VTA group*sex effect: $F_{1,75} = 4.29$, $P = 0.042$; SN group*sex effect: $F_{1,76} = 0.11$, $P = 0.75$; $N = 5$ animals/group/sex, 4 sections/animal). Post hoc comparisons of VTA data revealed significant differences between male CTR and SS DAT ($P = 0.039$) and TH ($P = 0.038$) intensity, but not between female CTR and SS (Fig. 2C, D). This was further confirmed by nested ANOVA analysis of DAT and TH immunoreactivity in male CTR and SS VTA (section(animal(group))): DAT $F_{1,50} = 12.48$, $P < 0.001$; TH $F_{1,30} = 18.26$, $P < 0.001$), demonstrating that SS induced down-regulation of DAT and TH fluorescence intensity in male VTA compared to CTR.

SS Reduces DAT Currents in the Developing Male VTA

To assess whether the DAT immunoreactivity reduction induced by SS in the male VTA was associated with changes in DAT-dependent currents, we performed electrophysiological recordings on individual DA neurons at PD22. We analyzed DA-induced DAT-mediated depolarizing currents in the lateral VTA. Using whole-cell voltage clamp recordings of individual DA neurons, we measured the amplitude of the inward current that developed in response to bath application of DA + sulpiride, a selective DRD2 antagonist, in midbrain slices. DA neurons of SS mice ($N = 10$ cells) displayed significant lower amplitudes of DAT dependent currents compared with CTR ($N = 12$ cells) (t -test: $t_{20} = -3.41$, $P = 0.0028$; $N = 3-4$ cells/animal, 3 animals/group; Fig. 2H, I).

Minocycline Treatment During SS Restores Morphology of Dopaminergic Neurons and Expression of DAT and TH in SS Male Mice

We have previously demonstrated that SS induces microglia activation in the VTA [22]. Pharmacological inhibition of SS-induced microglia activation by systemic administration

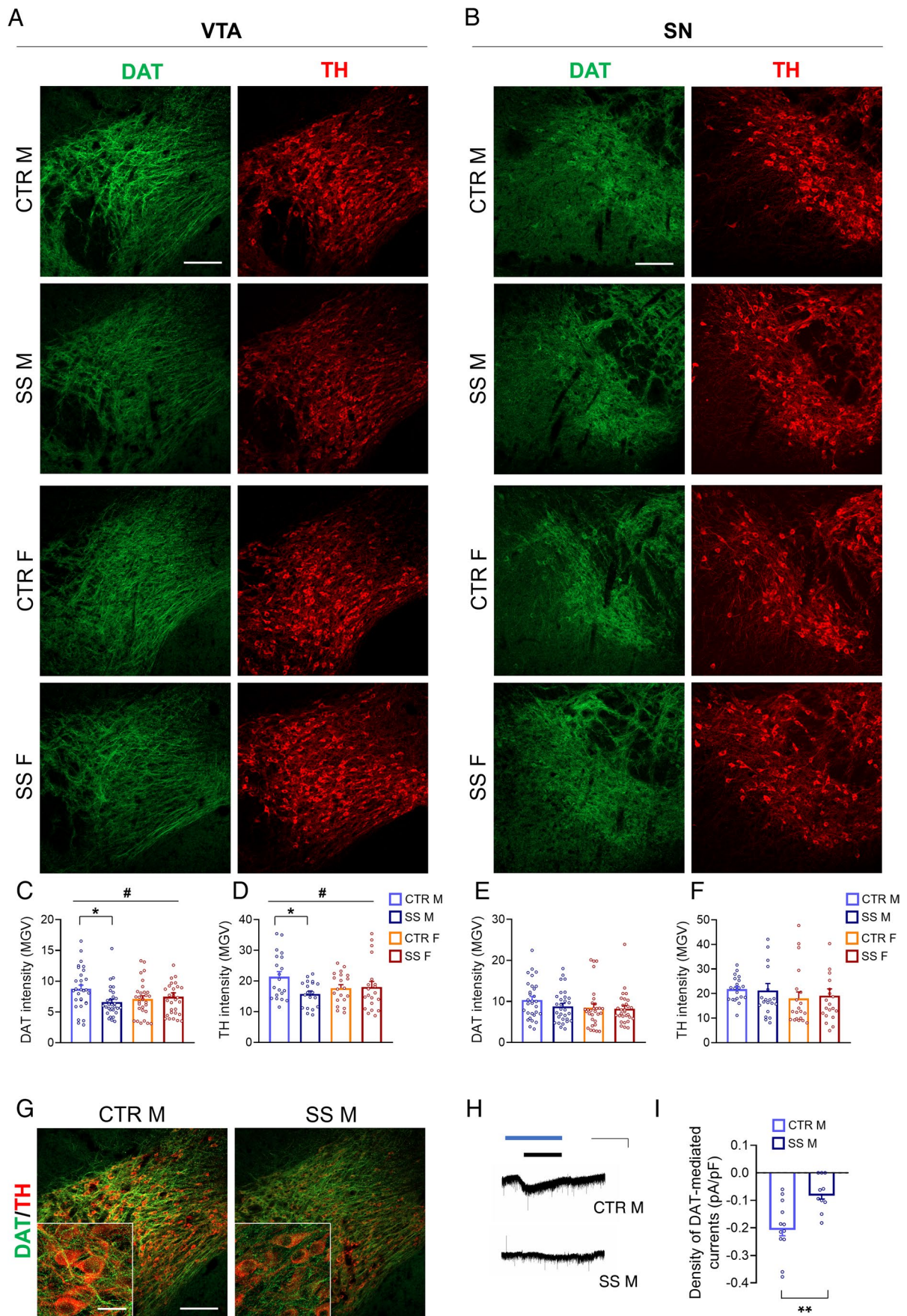


Fig. 2 SS downregulates dopaminergic markers in the developing VTA but not SN of male mice only. **A, B, G** Representative coronal hemisection images and **C–F** quantification of DAT and TH expression in the VTA and SN of female and male PD22 pups from CTR and SS groups as revealed by immunofluorescence and confocal microscopy. **C, D** DAT and TH intensity (reported as mean gray value, MGV) was significantly reduced in the VTA of male SS mice with respect to CTR, but not in female mice (two-way ANOVA, group*treatment effect: $P < 0.05$; Tukey HSD test: $P < 0.05$). **E, F** No significant stress effect was detected in female and male SN. **G** Representative confocal images of merged DAT and TH signals in the male VTA showing lower immunoreactivity and sparse signal distribution in SS mice compared to CTR. **H** Representative traces of DAT-mediated inward currents induced by bath application of dopamine (DA) (black bar, 30 μ M, 3 min) in the presence of sulpiride (blue bar, 5 μ M, 5 min), a selective DRD2 antagonist, recorded by means of whole-cell patch clamp ($V_h = -60$ mV) from VTA DA neurons of CTR and SS midbrain slices (scale bar = 3 min, 30 pA). **I** Mean density of DA-induced, DAT-mediated currents, expressed as percentage of control currents, shows lower current amplitudes in SS compared with CTR neurons at PD22 (t -test, $P < 0.01$). **C–F** $N = 5$ animals/group/sex; 4–6 hemisections/animal. Dots in the graphs represent average value for each section. Group*treatment effect: # $P < 0.05$; Tukey HSD test: * $P < 0.05$. **I** $N = 3$ animals/group; 3–4 cells/animal. Dots in the graphs represent average value for each cell. Student's t -test: ** $P < 0.01$. Data are presented as mean \pm s.e.m. Scale bars = (A, B, G) 100 μ m; (G inset) 20 μ m

of minocycline prevented emergence of dopaminergic electrophysiological alterations at PD22 and cocaine conditioned place preference in adult stressed mice. Here, we employed minocycline to explore if and how microglia contributed to the observed morphological and molecular dopaminergic alterations caused by ELS exposure in the VTA of male mice (Fig. 3A).

First, to evaluate whether developmental minocycline treatment alone had an effect on dopaminergic markers and microglia cell number in CTRs, we compared TH intensity and ionized calcium-binding adapter molecule 1 (Iba1, microglia/macrophages marker) expression in CTR-saline and CTR-minocycline male VTA at PD22. TH intensity and Iba1 + cell count were comparable between minocycline- and saline-injected mice (TH: t -test: $t_{31} = 1.42$, $P = 0.17$; Iba1 + cell count: t -test: $t_{31} = 1.58$, $P = 0.12$; Supplementary file1 Fig. 1A–C), further supporting the specificity of minocycline action on microglia activation only in the SS condition [22].

Thus, we proceeded by comparing CTR, SS, CTR-minocycline, and SS-minocycline mice to evaluate group (stress) and treatment (minocycline) effects. MANOVA of somatic indices showed a significant effect of group ($\lambda = 0.94$; $F_{2,115} = 3.90$; $P = 0.024$), treatment ($\lambda = 0.89$; $F_{2,115} = 7.10$; $P = 0.0011$), and group*treatment interaction ($\lambda = 0.89$; $F_{2,115} = 7.30$; $P < 0.001$). Univariate results indicated a significant group*treatment effect only on roundness ($F_{1,116} = 8.51$; $P = 0.0042$), but not on the aspect ratio ($F_{1,116} = 3.87$; $P = 0.052$, data not shown), and no main effect of group or treatment on either index. Post hoc comparisons confirmed significant differences in the roundness

only between CTR and SS untreated mice ($P = 0.012$), but no difference between the other groups, suggesting that roundness levels in SS-minocycline mice returned to CTR levels (Fig. 1B, F, CTR and SS: $N = 6$ animals/group, CTR-minocycline: $N = 3$ animals/group; SS-minocycline: $N = 5$ animals/group; all: 6 hemisections/animal).

Two-way ANOVA of DAT immunoreactivity showed a significant effect of group*treatment interaction ($F_{1,97} = 19.95$; $P < 0.001$), and no effect of the group or the treatment alone. Post hoc comparisons confirmed significant differences between CTR and SS untreated mice ($P = 0.035$), CTR-minocycline vs SS-minocycline ($P = 0.0037$), SS untreated vs SS-minocycline ($P < 0.001$), but no difference between CTR untreated and CTR-minocycline ($P = 0.33$), and in CTR untreated vs SS-minocycline ($P = 0.13$), indicating that minocycline treatment in SS mice restored immunoreactivity of DAT to CTR levels (Fig. 3C, G; CTR and SS: $N = 5$ animals/group, CTR-minocycline: $N = 3$ animals/group; SS-minocycline: $N = 4$ animals/group; 6 sections/animal).

Two-way ANOVA of TH immunoreactivity revealed significant main effect of group ($F_{1,63} = 6.12$, $P = 0.016$) and group*treatment interaction ($F_{1,63} = 36.55$, $P < 0.001$), but no effect of treatment alone. Post hoc comparisons showed significant differences between CTR and SS untreated mice ($P = 0.035$), CTR-minocycline vs SS-minocycline ($P < 0.001$), SS untreated vs SS-minocycline ($P < 0.001$), and CTR untreated vs SS-minocycline ($P = 0.0084$), indicating that minocycline treatment in SS mice (but not CTR mice) increased immunoreactivity of TH to levels above CTR (Fig. 3D, H; CTR and SS: $N = 5$ animals/group, CTR-minocycline: $N = 3$ animals/group; SS-minocycline: $N = 4$ animals/group; 4 sections/animal).

SS Alters Transcriptomic Patterning in the Developing Male VTA

To elucidate potential mechanisms involved in the effects of SS on the developing male VTA, we investigated molecular pathways globally modulated by SS by means of RNA-sequencing at the end of the stress procedure (Fig. 4A). Transcriptome analysis was performed by comparing 4 CTR and 4 SS male VTAs at PD 22. SS significantly ($padj < 0.05$) modulated 81 genes (Supplementary file2): 60 genes resulted downregulated in SS mice, while 21 were upregulated, as depicted in the heatmap (Fig. 4B) and volcano plot (Fig. 4C). Among the downregulated genes, 10 genes are crucial for dopaminergic functionality (Fig. 4D), with 9/10 taking part to the dopaminergic neurogenesis pathway (wikipathways.org/index.php/Pathway:WP1498), encompassing all the phases of neuronal development: the regionalization (engrailed homeobox 1 and 2, *En1* and *En2*), specification (aldehyde dehydrogenase 1 family member

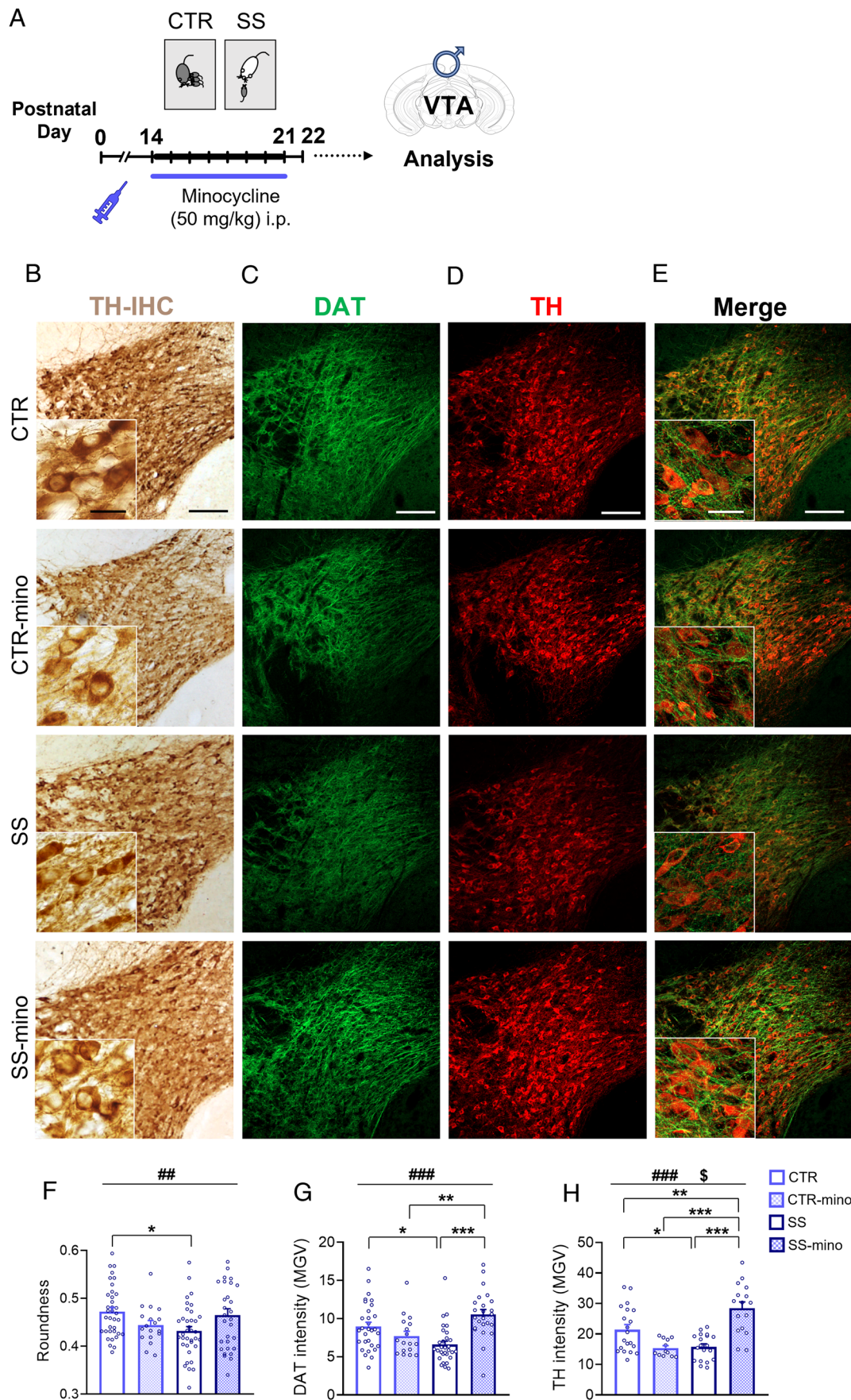


Fig. 3 Minocycline treatment reverts dopaminergic aberrations induced by SS. **A** Minocycline was daily administered through intraperitoneal (i.p.) injection to male CTR and SS mice from PD14 to 21. Analyses were performed in the VTA at PD22. **B–E** Lower and higher (insets) magnification of **B** TH-IHC stained neurons, and **C–E** DAT and TH immunofluorescence in the VTA (coronal hemisection) of CTR, CTR-minocycline (CTR-mino), SS, and SS-minocycline (SS-mino) male pups. **F** Minocycline in SS mice restored roundness of dopaminergic neurons to CTR levels (MANOVA univariate group*treatment effect, $P < 0.01$). **G, H** In SS-mino mice, DAT, and TH immunoreactivity were significantly increased with respect to SS mice, to levels comparable to or above CTR mice. **F** $N = 3–6$ animals/group; 6 hemisections/animal. Dots in the graphs represent average value for each hemisection. Univariate group*treatment effect: ## $P < 0.01$; Tukey HSD test: * $P < 0.05$. **G, H** $N = 3–5$ animals/group; 4–6 sections/animal. Dots in the graphs represent value for each section. Group*treatment effect: ### $P < 0.001$; group effect: \$ $P < 0.05$; Tukey HSD test: * $P < 0.05$, ** $P < 0.01$, *** $P < 0.001$. Data are presented as mean \pm s.e.m. Scale bars = (B–E) 100 μ m, (B, E insets) 20 μ m

A1), differentiation (*En1*; *En2*; paired like homeodomain 3, *Pitx3*) and maturation (tyrosine hydroxylase, *Th*; dopa decarboxylase, *Ddc*; dopamine transporter; vesicular monoamine transporter member 2; *Pitx3*; RET receptor tyrosine kinase). Moreover, some of these genes encode for proteins that are critical for dopamine metabolism, such as the TH and the DDC, and for dopamine activity, such as the DAT and the dopamine receptor D2, DRD2. Other highly significant downregulated genes include the GTP cyclohydrolase 1 gene (*Gch1*), responsible for the production of a TH cofactor, nicotinic cholinergic receptors (cholinergic receptor nicotinic alpha 4 subunit; cholinergic receptor nicotinic alpha 6 subunit; neuronal acetylcholine (nicotine) receptor subunit beta-3), genes associated with synaptic vesicle exocytosis such as complexin 1 and 2 genes, neuron-derived neurotrophic factor, and the peptide guanylate cyclase 2c (*Gucy2c*). Among the few upregulated genes, the most interesting targets were the corticotropin releasing hormone binding protein (*Crhbp*), the thyrotropin releasing hormone (*Trh*), and the neuropeptide neurokinin 2/alpha (tachykinin 2, *Tac2*) (Fig. 4C).

Ingenuity pathway analysis (IPA) software was used to determine the functional annotation and to predict the biological pathways affected by SS ($P < 0.05$). We focused on pathways associated with dopaminergic function, developmental processes, and neuro-psychological disorders. Significant diseases or functions annotations have been grouped on the basis of IPA categories in (Fig. 5A–C): Cell-to-cell signaling and interaction (A), nervous system development (B), and neurological disease, organismal injury and abnormalities, developmental, and psychological disorders (C). Based on the pathways predicted, SS broadly affects dopamine functionality, from the metabolism to the release and trafficking, and impairs neurotransmission (Fig. 5A). Moreover, SS influences developmental trajectories, affecting

neuronal formation, differentiation, and survival (Fig. 5B), possibly increasing susceptibility to neurological, psychological, and neurodevelopmental disorders (Fig. 5C). TOP predicted altered ingenuity canonical pathways (Fig. 5D) include dopamine and serotonin signaling, catecholamines biosynthesis, GPCR-mediated integration of enteroendocrine signaling exemplified by an L cell, tryptophan degradation X, and tetrahydrobiopterin biosynthesis I. Finally, gene ontology classification revealed alteration in hormonal-related biological processes, exocytosis, and synaptic vesicles trafficking (Fig. 5E).

Discussion

Stress in early life can disrupt trajectories of dopaminergic system maturation and increase susceptibility to psychopathology and neurological disorders, but the underlying mechanisms are still unknown. In this study, we showed that repeated social stress exposure early in life can alter the development of the DA system at the morphological, molecular, and electrophysiological level, in a sex- and region-dependent manner. Moreover, we showed for the first time an involvement of microglia/immune activity in the mediation of ELS effects on the DA system. Finally, we provided the first transcriptome analysis of the developing VTA immediately after ELS exposure, revealing a series of altered pathways that can be explored in future studies to unveil the biological processes underlying social stress response.

We found that, similarly to other ELS models, SS did not induce reduction in the number [56] and soma size [31] of dopaminergic neurons at PD22. However, we detected changes in the morphology of the dopaminergic cell body. Given that the neuronal soma hosts numerous processes involved in the maintenance of neuron functionality, morphological changes in this compartment may underlie a condition of altered homeostasis induced by the stressful stimulation [33, 57, 58]. Alternatively, since somatic shapes have been used to classify distinct subtypes of neurons [33] in other brain regions (e.g., pyramidal neurons in the cerebral cortex) [59], diverse distributions in shape profiles of DA cells from CTR and SS mice may be due to difference in dopaminergic subpopulations. However, morphological heterogeneity and its functional significance in VTA DA cells have not been characterized yet. In addition to DA cell body changes, SS induced a drastic reduction in the immunoreactivity of TH and DAT, along with decreased DAT currents. These observations confirm and expand literature findings demonstrating that ELS can alter the expression of such targets [11] and may suggest reduced DA synthesis and DAT-mediated responses to extracellular DA in VTA dopaminergic neurons from SS

Fig. 4 SS alters the transcriptome in the developing male VTA. **A** SS and CTR male VTA were collected at PD22 ($n=4/\text{group}$). The drawing shows the location of the punches (bilateral 0.5 mm circular sampling). RNA-sequencing revealed 81 differentially expressed genes (DEGs) between the two groups. **B** Heatmap and **C** volcano plot of the DEGs. Downregulated genes in SS are highlighted in blue and upregulated genes are red (p adjusted < 0.05). Not significantly modulated genes are shown in black. Selected genes of relevant pathways have been labeled. **D** Table with $\log_2(\text{fold change})$ values of dopaminergic DEGs and statistical significance (SS relative to CTR, p adjusted). *Slc6a3*, dopamine transporter; *Slc18a2*, vesicular monoamine transporter member 2; *Ddc*, dopa decarboxylase; *Th*, tyrosine hydroxylase; *Ret*, RET receptor tyrosine kinase; *Aldh1a1*, aldehyde dehydrogenase 1 family member A1; *En2*, engrailed homeobox 2; *Pitx3*, paired like homeodomain 3; *En1*, engrailed homeobox 1; *Drd2*, dopamine receptor D2; *Chrn3*, neuronal acetylcholine (nicotine) receptor subunit beta-3; *Gucy2c*, peptide guanylate cyclase 2c; *Chrna6*, cholinergic receptor nicotinic alpha 6 subunit; *Gch1*, GTP cyclohydrolase 1; *Ndnf*, neuron-derived neurotrophic factor; *Cplx1*, complexin 1; *Chrna4*, cholinergic receptor nicotinic alpha 4 subunit; *Cplx2*, complexin 2; *Trh*, thyrotropin releasing hormone; *Tac2*, tachykinin 2; *Crhbp*, corticotropin releasing hormone binding protein

mice. There is growing appreciation of the key role played by the DAT in midbrain regions, which is not only limited to reducing extracellular dopamine levels, but also includes regulation of dopaminergic network connectivity and plasticity [43, 60, 61]. DAT is found in the plasma membrane of the perikaryal, axon terminal, and dendrites of SN and VTA dopamine neurons [55, 62]. Within the midbrain, the extracellular levels of DA contribute to cell excitability and depend on a delicate interplay between DA somatodendritic release and DAT-mediated uptake [63]. Somatodendritic DA release, which is responsible for D2 autoreceptor self-inhibition, involves at least three different mechanisms. First, Ca^{2+} -dependent vesicular release of DA at low (5–10 nM) or high concentrations (150–400 nM) triggered by spontaneous pacemaker or bursting of VTA and SN DA neurons, respectively [64]. Secondly, other than clearing DA from extracellular space, DAT has been proposed to contribute to somatodendritic DA release via its reverse mode [65, 66]. Finally, in response to low DA concentrations (not enough to activate D2 autoreceptors), DAT-mediated uptake causes an excitatory current which contributes to increase action potential firing [43] and Ca^{2+} -dependent vesicular release of DA. In this regard, DAT has been considered as ionotropic receptor gated by DA and generating an inward current whose amplitude reflects the degree of its activation [67, 68]. We have previously shown that, at PD22, VTA DA neurons from SS mice displayed reduced self-inhibitory currents induced by exogenous DA application [22]. This reduction, which does not depend on DRD2 functionality [22], may be the result of a complex interaction between altered DAT currents and intracellular and extracellular mechanisms of DA regulation and response. Further studies are necessary to understand the mechanisms underlying

these findings and their functional implication on the dopaminergic circuit.

Interestingly, all these SS-induced dopaminergic effects observed at PD22 were present only in males. Current debates in neuroscience highlight the importance of considering “sex as a biological variable” in basic and translational research, particularly in the context of ELS, since male and female brains and bodies mature at different rates, and under different biological and environmental conditions [69, 70]. In humans, certain types of child maltreatment have been associated with different dimensions of psychopathology in men and women, and many psychiatric and neurological disorders show a sex bias in incidence, age of onset, and symptomatology, with increased incidence of neurodevelopmental disorders in boys, and of adolescent-onset mood disorders in girls [71–73]. Animal studies have confirmed sex-specific effects of ELS on neural and behavioral development [73, 74], with male offspring having greater risk of adverse proximal effects, as measured in proximity to the of pre-pubertal stress procedure (“within the same developmental epoch as the stress exposure”) [70]. Sex differences in the reward DA system may impact developmental trajectories and responses to stress [75, 76], and recent studies have shown opposite genome-wide signatures of response to ELS between adult female and male VTA [77–79]. Moreover, male and female dopaminergic systems are differentially sculpted by microglia during adolescence [16]. Notably, early postnatal/adolescent stress and early immune activation seem to induce greater neuroimmunological responses in males than in females [80]. In the light of this evidence, it can be hypothesized that the specific male response to SS that we detected may be due to higher sensitivity of the dopaminergic and/or immune system in males compared to females during this developmental window, and/or to sex-different timing in brain responses to stress, which in males may be expressed in proximity to the stress. Further studies are needed to investigate whether SS affects female VTA and/or other brain regions at different time points across the life span.

Consistent with previous literature [11], we detected a regional effect in the dopaminergic responses to SS, with changes being significant in the VTA but not in the SN. Indeed, VTA DA neurons are known to be particularly responsive to “psychological”/behavioral stressors [28, 53, 81], and express higher levels of transcripts related to synaptic plasticity and neuropeptides compared to the SN [82]. The sensitivity of the VTA may be also due to specific neuron-microglia communication, since VTA microglia is prominently different from other basal ganglia, namely nucleus accumbens, cortex and SN microglia [83].

We found that inhibition of SS-induced microglia/immune activation through minocycline prevented some alterations in the morphology of DA neurons and DAT

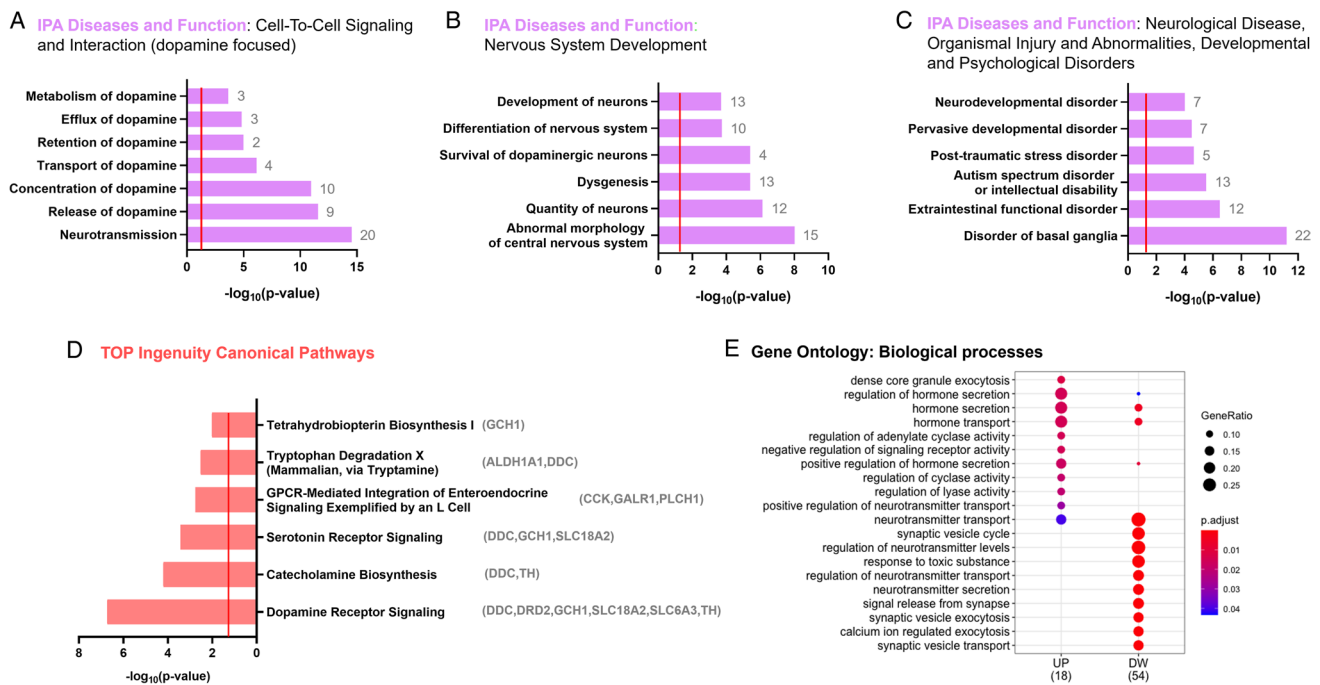


Fig. 5 Gene set enrichment analysis of the differentially expressed genes reveals altered developmental trajectories and signaling following SS. **A–C** Selected predicted diseases and function annotations affected by SS as revealed by ingenuity pathway analysis (IPA). Annotations are grouped in IPA categories including **A** cell-to-cell signaling and interaction, **B** nervous system development, and **C** neurological disease, organismal injury and abnormalities, developmental and psychological disorders. The number of DEGs relating to each

term is provided next to the corresponding bar. **D** Predicted altered ingenuity canonical pathways in SS mice vs CTR with relative DEGs. **E** Dot blot of the TOP 10 enriched up (UP) and downregulated (DW) gene ontology biological processes terms of the DEGs. The size of the dots is based on gene counts enriched in the pathway, while the color shows pathway enrichment significance as indicated in the legend. **A–D** The red line indicates $P=0.05$

and TH levels in the VTA of male SS mice. Therefore, it is plausible to suggest a role for neuroimmune pathways in the regulation of SS-induced altered development of the DA system. Disentangling neuroimmune pathways is incredibly challenging, and in our setting, it is even more so because minocycline mechanism of action is still not well known. However, minocycline has been extensively used to specifically inhibit microglia activation in response to a variety of different stimuli [26, 84–86], with similar results to more specific compounds (e.g., PLX3397, GW2580) [22, 87]. In microglia, minocycline is known to prevent/reduce stimulus-induced proliferation, production of proinflammatory mediators, phagocytic activity, and morphological and molecular shifts associated with a reactive phenotype [84, 85, 88]. Moreover, it has beneficial effects on dopaminergic neurotoxicity, neuronal apoptotic mechanisms, oxidative stress, glutamate dysfunction, and peripheral inflammation, all processes that influence and are influenced by microglia [84, 89, 90]. Importantly, minocycline effects on microglia and the dopaminergic system may also be the result of inhibited peripheral immune responses, which are known to play a central role in psychosocial stress response [91, 92].

To unravel possible pathways of SS response, we performed RNA-sequencing in the male developing VTA (PD22) at the end of the stress procedure. Our transcriptome analysis confirmed massive downregulation of numerous dopaminergic markers, including TH and DAT genes, and alterations in pathways involved in the synthesis, signaling, and degradation of DA. This effect is not a consequence of reduction in dopaminergic neurons, as CTR and SS mice exhibit the same number of DA cells in the VTA, but it is probably due to transcriptional regulation processes that ultimately affect protein expression, as we demonstrated for TH and DAT. Furthermore, pathway analysis predicted alterations associated with neurodevelopmental trajectories and neurological and psychiatric disorders. Overall, transcriptome, immunohistochemical, and electrophysiological data suggest that SS interferes with developmental programs of the male VTA, possibly inducing diminished DA signaling at the end of the ELS procedure (PD22). Reduction of DA function may be an adaptive response to the repeated, inescapable stress that pups face [93]. It has been shown that DA transmission between the third and fourth postnatal week is critical for the maturation of DA circuitry [94], and developmental DA perturbation has been associated with

altered behavioral phenotypes that resemble mental disorders (e.g., attention deficit hyperactivity disorder, substance use disorders [9, 14, 95]). In clinical research, aberrant VTA maturation has been observed in children and adolescent exposed to early life stress or trauma [81, 96].

Microglia and immune pathways may be important regulators of the observed dopaminergic effects, since minocycline was able to rescue the deficits in DAT and TH induced by SS. It has been shown that immune-derived cytokines and prostaglandins cause reductions in DA synthesis, release, and DA metabolites, possibly via depletion of tetrahydrobiopterin (BH4), the cofactor of phenylalanine hydroxylase and TH [97–99]. This neuroimmune pathway has been proposed as the underlying mechanism in inflammation-induced psychiatric symptoms associated with impaired dopamine transmission, such as anhedonia [97, 100, 101]. Interestingly, our RNA-seq revealed alteration of the tetrahydrobiopterin biosynthesis I pathway in SS mice, due to the reduction in the *Gch1* gene, the rate-limiting enzyme in the production of BH4 [102] whose deficiency has been associated with dopaminergic-related diseases, including Parkinson's disease [103]. Additionally, a highly significant modulation of genes and pathways associated with cholinergic and serotonergic transmission suggests the presence of complex local interactions between different neurotransmitter systems underlying VTA SS response.

Among the few upregulated pathways, we found hormonal and peptide signaling pathways. The related DEGs include markers that are canonically involved in hypothalamic–pituitary–adrenal axis–VTA responses to stress and drugs of abuse, such as *Crhbp* [13], and new targets that merit further consideration. For example, we found strong upregulation of the *Tac2* and *Trh* genes. *Tac2* is upregulated in the brain after chronic social isolation stress [104], and its downstream pathways can affect dopaminergic release from the VTA [105]. *Trh* is involved in the regulation and release of thyroid-stimulating hormone (thyrotropin) and prolactin from the pituitary gland. In the VTA, it is possibly expressed by a sub-group of GABA and/or glutamate neurons or coming from hypothalamic afferent fibers [106]. TRH seems to be involved in regulating behavioral, energy, and immune homeostasis in the periphery and the brain, including the ventral midbrain, where it exerts a neuroprotective role under oxidative stress conditions in dopaminergic neurons [107]. Moreover, thyroid hormone and associated proteins have recently been implicated in regulation of sex-specific neurodevelopment and response to adolescent stress in animals, and post-traumatic stress disorder in humans [78, 108, 109]. A significantly downregulated neuropeptide gene is *Gucy2c*, which encodes a transmembrane receptor for the intestinal hormone uroguanylin that takes part in the gut-brain endocrine axis regulation of feeding behavior. In the brain, it is selectively expressed by the hypothalamus and

dopaminergic neurons from the VTA and SN and distributed in their afferent sites [110]. It is involved in the development of chronic defeat stress-induced depressive behavior and its substrate uroguanylin is decreased peripherally in socially defeated mice [111, 112]. Intriguingly, IPA analysis revealed enrichment in the extraintestinal functional disorder and GPCR-mediated integration of enteroendocrine signaling exemplified by L cell pathways. The genes within our dataset relating to these pathways encode for peptides found in the gut and in the brain and involved in gut-brain communication, neurodevelopment, and behavior [113–116].

In light of these results, we speculate that during social stress exposure, the VTA may be a station where neurotransmitters, hormones, peptides, and immune molecules signal internal homeostatic states from the brain and the periphery to influence central dopaminergic neurotransmission and establish appropriate learning and predictions [98, 117]. This, in turn, would affect future emotional/motivational behavioral choices, which in the case of chronic stress may be maladaptive and increase psychopathological risk [53]. In this setting, microglia would play a central role, since they can sense and read all the signals coming from nervous and peripheral tissues [118]. It can be hypothesized that SS-stimulated microglia mount an inflammatory response that would end up negatively contributing to the observed dopamine neuron changes and DA reduction in SS male VTA. Unfortunately, several technical issues did not allow us to better explore microglia contribution. In particular, the mouse strain employed in this study (DBA/2) made it impossible to take advantage of genetic mouse models of microglia tagging and manipulation, which are based on the C57BL/6 strain. This, in combination with the small size of the developing mouse VTA, meant that we were not able to extract vital microglia cells that could be employed for transcriptomic or in vitro studies. Validation of the SS model on the C57BL/6 strain will prove instrumental to investigations of the specific role of microglia in this setting.

A possible limitation of the study concerns the fact that we stopped analyzing females after we detected significant effects only in males. Including female mice in subsequent experiments (minocycline treatment, RNA-sequencing) would have been advantageous to better explore the observed sex differences and to draw more reliable conclusions on the potential of minocycline to prevent SS-induced dopaminergic aberrations. Future efforts should be made to address this limitation, and to detect which brain substrates are affected by SS in female mice at different developmental time points, in order to provide better knowledge on possible sex-specific pathophysiology in chronic medical conditions.

Overall, these results suggest important targets of developmental repeated social stress effects, with sex and regional specificity, and involvement of microglia and immune system in the mediation of these effects. Additional investigations are

needed to evaluate whether the SS-induced developmental dopaminergic alterations described here are maintained in adulthood, or whether different adaptations will occur in the system, and the possible causal relationship with psychopathological risk. A better understanding of such pathways is critical for improving strategies that counteract aberrant brain maturation and psychopathological outcomes following adverse early experiences.

Supplementary Information The online version contains supplementary material available at <https://doi.org/10.1007/s12035-022-02830-6>.

Acknowledgements We thank Stephen Girona for helping with the experiments and Rhys David Talbot for editing an English draft of this manuscript.

Author Contribution C.C. contributed experimental design, behavior, immunohistochemistry, RNA extraction, statistical analysis, interpretation of data, and writing of manuscript. L.L.I. contributed experimental design, feedback, and funding acquisition. A.M., E.G., and N.B.M. contributed electrophysiological experiment and interpretation, funding acquisition, and resources. C.H. contributed RNA-sequencing analysis and visualization. M.T.V. contributed feedback, funding acquisition, and resources. D.P. contributed funding acquisition, supervision of the interpretation, analysis, and visualization of the RNA-sequencing. V.C. contributed experimental design, supervision, statistical analysis, funding acquisition, interpretation of data, and writing of manuscript.

Funding Open access funding provided by Università degli Studi di Roma La Sapienza within the CRUI-CARE Agreement. This work was supported by the Italian Ministry of Health Young Researcher Grant (GR-2009–1576820) to V.C., Sapienza University of Rome Avvio alla Ricerca 2019 (AR11916B88FCD3DC) to C.C., Università Cattolica del S. Cuore Linea D.1. 2019–20 to M.T.V., and University of Naples Parthenope 'Ricerca Competitiva di Ateneo N. DSTE 315A' to E.G.

Data Availability All source data supporting the findings of this manuscript are available from first and corresponding authors upon request. RNA-Seq data are available through NCBI's Gene Expression Omnibus (GEO) repository, under accession number GSE199136.

Declarations

Ethics Approval All experiments were carried out in accordance with Italian national law (DL 26/2014) on the use of animals for research based on the European Communities Council Directive (2010/63/UE) and comply with the ARRIVE guidelines. Experiments were approved by the ethics committee of the Italian Ministry of Health (license/approval IDs: #42/2015-PR; #677/2019-PR) and by local Ethical Committee of the Santa Lucia Foundation. All efforts were made to minimize the number of animals used and their suffering.

Consent to Participate Not applicable.

Consent for Publication Not applicable.

Competing Interests The authors declare no competing interests.

This article is licensed under a Creative Commons Attribution 4.0 International License, which permits use, sharing, adaptation, distribution and reproduction in any medium or format, as long as you

give appropriate credit to the original author(s) and the source, provide a link to the Creative Commons licence, and indicate if changes were made. The images or other third party material in this article are included in the article's Creative Commons licence, unless indicated otherwise in a credit line to the material. If material is not included in the article's Creative Commons licence and your intended use is not permitted by statutory regulation or exceeds the permitted use, you will need to obtain permission directly from the copyright holder. To view a copy of this licence, visit <http://creativecommons.org/licenses/by/4.0/>.

References

- Teicher MH, Samson JA, Anderson CM, Ohashi K (2016) The effects of childhood maltreatment on brain structure, function and connectivity. *Nat Rev Neurosci* 17:652–666. <https://doi.org/10.1038/nrn.2016.111>
- Short AK, Baram TZ (2019) Early-life adversity and neurological disease: age-old questions and novel answers. *Nat Rev Neurol* 15:657–669. <https://doi.org/10.1038/s41582-019-0246-5>
- Herzberg MP, Gunnar MR (2020) Early life stress and brain function: activity and connectivity associated with processing emotion and reward. *Neuroimage* 209:116493. <https://doi.org/10.1016/j.neuroimage.2019.116493>
- Novick AM, Levandowski ML, Laumann LE et al (2018) The effects of early life stress on reward processing. *J Psychiatr Res* 101:80–103. <https://doi.org/10.1016/j.jpsychires.2018.02.002>
- Birn RM, Roeber BJ, Pollak SD (2017) Early childhood stress exposure, reward pathways, and adult decision making. *Proc Natl Acad Sci U S A* 114:13549–13554. <https://doi.org/10.1073/pnas.1708791114>
- Gatzke-Kopp LM (2011) The canary in the coalmine: the sensitivity of mesolimbic dopamine to environmental adversity during development. *Neurosci Biobehav Rev* 35:794–803. <https://doi.org/10.1016/j.neubiorev.2010.09.013>
- Money KM, Stanwood GD (2013) Developmental origins of brain disorders: roles for dopamine. *Front Cell Neurosci* 7:260. <https://doi.org/10.3389/fncel.2013.00260>
- Russo SJ, Nestler EJ (2013) The brain reward circuitry in mood disorders. *Nat Rev Neurosci* 14:609–625. <https://doi.org/10.1038/nrn3381>
- Levis SC, Baram TZ, Mahler SV (2021) Neurodevelopmental origins of substance use disorders: Evidence from animal models of early-life adversity and addiction. *Eur J Neurosci*. <https://doi.org/10.1111/ejn.15223>
- Nelson CA, Scott RD, Bhutta ZA et al (2020) Adversity in childhood is linked to mental and physical health throughout life. *BMJ* 371:m3048. <https://doi.org/10.1136/bmj.m3048>
- Rodrigues A-J, Leão P, Carvalho M et al (2011) Potential programming of dopaminergic circuits by early life stress. *Psychopharmacology* 214:107–120. <https://doi.org/10.1007/s00213-010-2085-3>
- Coque L, Mukherjee S, Cao J-L et al (2011) Specific role of VTA dopamine neuronal firing rates and morphology in the reversal of anxiety-related, but not depression-related behavior in the ClockΔ19 mouse model of mania. *Neuropsychopharmacology* 36:1478–1488. <https://doi.org/10.1038/npp.2011.33>
- Burke AR, Miczek KA (2014) Stress in adolescence and drugs of abuse in rodent models: role of dopamine, CRF, and HPA axis. *Psychopharmacology* 231:1557–1580. <https://doi.org/10.1007/s00213-013-3369-1>
- Suri D, Teixeira CM, Caghiostro MKC et al (2015) Monoamine-sensitive developmental periods impacting adult emotional and cognitive behaviors. *Neuropsychopharmacology* 40:88–112. <https://doi.org/10.1038/npp.2014.231>

15. Squarzone P, Oller G, Hoeffel G et al (2014) Microglia modulate wiring of the embryonic forebrain. *Cell Rep* 8:1271–1279. <https://doi.org/10.1016/j.celrep.2014.07.042>
16. Kopec AM, Smith CJ, Ayre NR et al (2018) Microglial dopamine receptor elimination defines sex-specific nucleus accumbens development and social behavior in adolescent rats. *Nat Commun* 9:3769. <https://doi.org/10.1038/s41467-018-06118-z>
17. Danese A, Baldwin JR (2017) Hidden wounds? Inflammatory links between childhood trauma and psychopathology. *Annu Rev Psychol* 68:517–544. <https://doi.org/10.1146/annurev-psych-010416-044208>
18. Catale C, Gironda S, Lo Iacono L, Carola V (2020) Microglial function in the effects of early-life stress on brain and behavioral development. *J Clin Med* 9. <https://doi.org/10.3390/jcm9020468>
19. Johnson FK, Kaffman A (2018) Early life stress perturbs the function of microglia in the developing rodent brain: new insights and future challenges. *Brain Behav Immun* 69:18–27. <https://doi.org/10.1016/j.bbi.2017.06.008>
20. Catale C, Bisicchia E, Carola V, Viscomi MT (2021) Early life stress exposure worsens adult remote microglia activation, neuronal death, and functional recovery after focal brain injury. *Brain Behav Immun* 94:89–103. <https://doi.org/10.1016/j.bbi.2021.02.032>
21. Lo Iacono L, Valzania A, Visco-Comandini F et al (2017) Social threat exposure in juvenile mice promotes cocaine-seeking by altering blood clotting and brain vasculature. *Addict Biol* 22:911–922. <https://doi.org/10.1111/adb.12373>
22. Lo Iacono L, Catale C, Martini A et al (2018) From traumatic childhood to cocaine abuse: the critical function of the immune system. *Biol Psychiatry* 84:905–916. <https://doi.org/10.1016/j.biopsych.2018.05.022>
23. Lo Iacono L, Valzania A, Visco-Comandini F et al (2016) Regulation of nucleus accumbens transcript levels in mice by early-life social stress and cocaine. *Neuropharmacology* 103:183–194. <https://doi.org/10.1016/j.neuropharm.2015.12.011>
24. Valzania A, Catale C, Viscomi MT et al (2017) Histone deacetylase 5 modulates the effects of social adversity in early life on cocaine-induced behavior. *Physiol Behav* 171:7–12. <https://doi.org/10.1016/j.physbeh.2016.12.027>
25. Catale C, Bussone S, Lo Iacono L et al (2020) Exposure to different early-life stress experiences results in differentially altered DNA methylation in the brain and immune system. *Neurobiol Stress* 13:100249. <https://doi.org/10.1016/j.ynstr.2020.100249>
26. Fan R, Xu F, Previti ML et al (2007) Minocycline reduces microglial activation and improves behavioral deficits in a transgenic model of cerebral microvascular amyloid. *J Neurosci* 27:3057–3063. <https://doi.org/10.1523/JNEUROSCI.4371-06.2007>
27. Paxinos G, Franklin KBJ (2001) The mouse brain in stereotaxic coordinates, 2nd edn. Academic Press, San Diego
28. Holly EN, Miczek KA (2016) Ventral tegmental area dopamine revisited: effects of acute and repeated stress. *Psychopharmacology* 233:163–186. <https://doi.org/10.1007/s00213-015-4151-3>
29. Morales M, Margolis EB (2017) Ventral tegmental area: cellular heterogeneity, connectivity and behaviour. *Nat Rev Neurosci* 18:73–85. <https://doi.org/10.1038/nrn.2016.165>
30. Nobili A, Latagliata EC, Viscomi MT et al (2017) Dopamine neuronal loss contributes to memory and reward dysfunction in a model of Alzheimer's disease. *Nat Commun* 8:14727. <https://doi.org/10.1038/ncomms14727>
31. Chocyk A, Przyborowska A, Dudys D et al (2011) The impact of maternal separation on the number of tyrosine hydroxylase-expressing midbrain neurons during different stages of ontogenesis. *Neuroscience* 182:43–61. <https://doi.org/10.1016/j.neuroscience.2011.03.008>
32. Latini L, Bisicchia E, Sasso V et al (2014) Cannabinoid CB2 receptor (CB2R) stimulation delays rubrospinal mitochondrial-dependent degeneration and improves functional recovery after spinal cord hemisection by ERK1/2 inactivation. *Cell Death Dis* 5:e1404. <https://doi.org/10.1038/cddis.2014.364>
33. Meijering E (2010) Neuron tracing in perspective. *Cytometry A* 77:693–704. <https://doi.org/10.1002/cyto.a.20895>
34. Schneider CA, Rasband WS, Eliceiri KW (2012) NIH Image to ImageJ: 25 years of image analysis. *Nat Methods* 9:671–675. <https://doi.org/10.1038/nmeth.2089>
35. D'Addario SL, Di Segni M, Ledonne A et al (2021) Resilience to anhedonia-passive coping induced by early life experience is linked to a long-lasting reduction of I(h) current in VTA dopaminergic neurons. *Neurobiol Stress* 14:100324. <https://doi.org/10.1016/j.ynstr.2021.100324>
36. Krashia P, Martini A, Nobili A et al (2017) On the properties of identified dopaminergic neurons in the mouse substantia nigra and ventral tegmental area. *Eur J Neurosci* 45:92–105. <https://doi.org/10.1111/ejn.13364>
37. Chieng B, Azriel Y, Mohammadi S, Christie MJ (2011) Distinct cellular properties of identified dopaminergic and GABAergic neurons in the mouse ventral tegmental area. *J Physiol* 589:3775–3787. <https://doi.org/10.1113/jphysiol.2011.210807>
38. Mercuri NB, Bonci A, Calabresi P et al (1995) Properties of the hyperpolarization-activated cation current Ih in rat midbrain dopaminergic neurons. *Eur J Neurosci* 7:462–469. <https://doi.org/10.1111/j.1460-9568.1995.tb00342.x>
39. Kilty JE, Lorang D, Amara SG (1991) Cloning and expression of a cocaine-sensitive rat dopamine transporter. *Science* 254:578–579. <https://doi.org/10.1126/science.1948035>
40. Gu H, Wall SC, Rudnick G (1994) Stable expression of biogenic amine transporters reveals differences in inhibitor sensitivity, kinetics, and ion dependence. *J Biol Chem* 269:7124–7130
41. Mortensen OV, Amara SG (2003) Dynamic regulation of the dopamine transporter. *Eur J Pharmacol* 479:159–170. <https://doi.org/10.1016/j.ejphar.2003.08.066>
42. Vaughan RA, Foster JD (2013) Mechanisms of dopamine transporter regulation in normal and disease states. *Trends Pharmacol Sci* 34:489–496. <https://doi.org/10.1016/j.tips.2013.07.005>
43. Ingram SL, Prasad BM, Amara SG (2002) Dopamine transporter-mediated conductances increase excitability of midbrain dopamine neurons. *Nat Neurosci* 5:971–978. <https://doi.org/10.1038/nn920>
44. Carvelli L, McDonald PW, Blakely RD, DeFelice LJ (2004) Dopamine transporters depolarize neurons by a channel mechanism. *Proc Natl Acad Sci U S A* 101:16046–16051. <https://doi.org/10.1073/pnas.0403299101>
45. Branch SY, Beckstead MJ (2012) Methamphetamine produces bidirectional, concentration-dependent effects on dopamine neuron excitability and dopamine-mediated synaptic currents. *J Neurophysiol* 108:802–809. <https://doi.org/10.1152/jn.00094.2012>
46. Guatteo E, Yee A, McKearney J et al (2013) Dual effects of L-DOPA on nigral dopaminergic neurons. *Exp Neurol* 247:582–594. <https://doi.org/10.1016/j.expneurol.2013.02.009>
47. Ventura R, Cabib S, Puglisi-Allegra S (2002) Genetic susceptibility of mesocortical dopamine to stress determines liability to inhibition of mesoaccumbens dopamine and to behavioral “despair” in a mouse model of depression. *Neuroscience* 115:999–1007. [https://doi.org/10.1016/s0306-4522\(02\)00581-x](https://doi.org/10.1016/s0306-4522(02)00581-x)
48. Love MI, Huber W, Anders S (2014) Moderated estimation of fold change and dispersion for RNA-seq data with DESeq2. *Genome Biol* 15:550. <https://doi.org/10.1186/s13059-014-0550-8>
49. Yu G, He Q-Y (2016) ReactomePA: an R/Bioconductor package for reactome pathway analysis and visualization. *Mol Biosyst* 12:477–479. <https://doi.org/10.1039/c5mb00663e>

50. Yu G, Wang L-G, Yan G-R, He Q-Y (2015) DOSE: an R/Bio-conductor package for disease ontology semantic and enrichment analysis. *Bioinformatics* 31:608–609. <https://doi.org/10.1093/bioinformatics/btu684>
51. Krzywinski M, Altman N, Blainey P (2014) Points of significance: nested designs. For studies with hierarchical noise sources, use a nested analysis of variance approach. *Nat Methods* 11:977–978. <https://doi.org/10.1038/nmeth.3137>
52. Oo TF, Burke RE (1997) The time course of developmental cell death in phenotypically defined dopaminergic neurons of the substantia nigra. *Brain Res Dev Brain Res* 98:191–196. [https://doi.org/10.1016/s0165-3806\(96\)00173-3](https://doi.org/10.1016/s0165-3806(96)00173-3)
53. Douma EH, de Kloet ER (2020) Stress-induced plasticity and functioning of ventral tegmental dopamine neurons. *Neurosci Biobehav Rev* 108:48–77. <https://doi.org/10.1016/j.neubiorev.2019.10.015>
54. Mazei-Robison MS, Koo JW, Friedman AK et al (2011) Role for mTOR signaling and neuronal activity in morphine-induced adaptations in ventral tegmental area dopamine neurons. *Neuron* 72:977–990. <https://doi.org/10.1016/j.neuron.2011.10.012>
55. Nirenberg MJ, Chan J, Vaughan RA et al (1997) Immunogold localization of the dopamine transporter: an ultrastructural study of the rat ventral tegmental area. *J Neurosci* 17:4037–4044. <https://doi.org/10.1523/JNEUROSCI.17-11-04037.1997>
56. Peña CJ, Kronman HG, Walker DM et al (2017) Early life stress confers lifelong stress susceptibility in mice via ventral tegmental area OTX2. *Science* 356:1185–1188. <https://doi.org/10.1126/science.aan4491>
57. Cai Q, Zakaria HM, Simone A, Sheng Z-H (2012) Spatial parkin translocation and degradation of damaged mitochondria via mitophagy in live cortical neurons. *Curr Biol* 22:545–552. <https://doi.org/10.1016/j.cub.2012.02.005>
58. Donato A, Kagias K, Zhang Y, Hilliard MA (2019) Neuronal sub-compartmentalization: a strategy to optimize neuronal function. *Biol Rev Camb Philos Soc* 94:1023–1037. <https://doi.org/10.1111/brv.12487>
59. Kasper EM, Larkman AU, Lübke J, Blakemore C (1994) Pyramidal neurons in layer 5 of the rat visual cortex. I. Correlation among cell morphology, intrinsic electrophysiological properties, and axon targets. *J Comp Neurol* 339:459–474. <https://doi.org/10.1002/cne.903390402>
60. Bu M, Farrer MJ, Khoshbouei H (2021) Dynamic control of the dopamine transporter in neurotransmission and homeostasis. *NPJ Parkinsons Dis* 7:22. <https://doi.org/10.1038/s41531-021-00161-2>
61. Miller DR, Guenther DT, Maurer AP et al (2021) Dopamine transporter is a master regulator of dopaminergic neural network connectivity. *J Neurosci* 41:5453–5470. <https://doi.org/10.1523/JNEUROSCI.0223-21.2021>
62. Ciliax BJ, Heilman C, Demchyshyn LL et al (1995) The dopamine transporter: immunochemical characterization and localization in brain. *J Neurosci* 15:1714–1723. <https://doi.org/10.1523/JNEUROSCI.15-03-01714.1995>
63. Hoffman AF, Lupica CR, Gerhardt GA (1998) Dopamine transporter activity in the substantia nigra and striatum assessed by high-speed chronoamperometric recordings in brain slices. *J Pharmacol Exp Ther* 287:487–496
64. Schultz W (1998) Predictive reward signal of dopamine neurons. *J Neurophysiol* 80:1–27. <https://doi.org/10.1152/jn.1998.80.1.1>
65. Falkenburger BH, Barstow KL, Mintz IM (2001) Dendroendritic inhibition through reversal of dopamine transport. *Science* 293:2465–2470. <https://doi.org/10.1126/science.1060645>
66. Guatteo E, Rizzo FR, Federici M et al (2017) Functional alterations of the dopaminergic and glutamatergic systems in spontaneous α -synuclein overexpressing rats. *Exp Neurol* 287:21–33. <https://doi.org/10.1016/j.expneurol.2016.10.009>
67. De Felice LJ (2017) Monoamine transporters as ionotropic receptors. *Trends Neurosci* 40:195–196. <https://doi.org/10.1016/j.tins.2017.02.003>
68. Aversa D, Martini A, Guatteo E et al (2018) Reversal of dopamine-mediated firing inhibition through activation of the dopamine transporter in substantia nigra pars compacta neurons. *Br J Pharmacol* 175:3534–3547. <https://doi.org/10.1111/bph.14422>
69. White JD, Kaffman A (2019) The moderating effects of sex on consequences of childhood maltreatment: from clinical studies to animal models. *Front Neurosci* 13:1082. <https://doi.org/10.3389/fnins.2019.01082>
70. Hodes GE, Epperson CN (2019) Sex differences in vulnerability and resilience to stress across the life span. *Biol Psychiatry* 86:421–432. <https://doi.org/10.1016/j.biopsych.2019.04.028>
71. Keyes KM, Eaton NR, Krueger RF et al (2012) Childhood maltreatment and the structure of common psychiatric disorders. *Br J Psychiatry* 200:107–115. <https://doi.org/10.1192/bjp.bp.111.093062>
72. Gegenhuber B, Tollkuhn J (2020) Signatures of sex: sex differences in gene expression in the vertebrate brain. *Wiley Interdiscip Rev Dev Biol* 9:e348. <https://doi.org/10.1002/wdev.348>
73. Bath KG (2020) Synthesizing views to understand sex differences in response to early life adversity. *Trends Neurosci* 43:300–310. <https://doi.org/10.1016/j.tins.2020.02.004>
74. Demaestri C, Pan T, Critz M et al (2020) Type of early life adversity confers differential, sex-dependent effects on early maturational milestones in mice. *Horm Behav* 124:104763. <https://doi.org/10.1016/j.yhbeh.2020.104763>
75. Gillies GE, Virdee K, McArthur S, Dalley JW (2014) Sex-dependent diversity in ventral tegmental dopaminergic neurons and developmental programming: a molecular, cellular and behavioral analysis. *Neuroscience* 282:69–85. <https://doi.org/10.1016/j.neuroscience.2014.05.033>
76. Trainor BC (2011) Stress responses and the mesolimbic dopamine system: social contexts and sex differences. *Horm Behav* 60:457–469. <https://doi.org/10.1016/j.yhbeh.2011.08.013>
77. Peña CJ, Smith M, Ramakrishnan A et al (2019) Early life stress alters transcriptomic patterning across reward circuitry in male and female mice. *Nat Commun* 10:5098. <https://doi.org/10.1038/s41467-019-13085-6>
78. Parel ST, Peña CJ (2020) Genome-wide signatures of early-life stress: influence of sex. *Biol Psychiatry*. <https://doi.org/10.1016/j.biopsych.2020.12.010>
79. Walker DM, Zhou X, Cunningham AM et al (2021) Sex-specific transcriptional changes in response to adolescent social stress in the brain's reward circuitry. *Biol Psychiatry*. <https://doi.org/10.1016/j.biopsych.2021.02.064>
80. Brydges NM, Reddaway J (2020) Neuroimmunological effects of early life experiences. *Brain Neurosci Adv* 4:2398212820953706. <https://doi.org/10.1177/2398212820953706>
81. Marusak HA, Hatfield JRB, Thomason ME, Rabinak CA (2017) Reduced ventral tegmental area-hippocampal connectivity in children and adolescents exposed to early threat. *Biol Psychiatry Cogn Neurosci Neuroimaging* 2:130–137. <https://doi.org/10.1016/j.bpsc.2016.11.002>
82. Greene JG (2006) Gene expression profiles of brain dopamine neurons and relevance to neuropsychiatric disease. *J Physiol* 575:411–416. <https://doi.org/10.1113/jphysiol.2006.112599>
83. De Biase LM, Schuebel KE, Fuschfeld ZH et al (2017) Local cues establish and maintain region-specific phenotypes of basal ganglia microglia. *Neuron* 95:341–356.e6. <https://doi.org/10.1016/j.neuron.2017.06.020>

84. Garrido-Mesa N, Zarzuelo A, Gálvez J (2013) What is behind the non-antibiotic properties of minocycline? *Pharmacol Res* 67:18–30. <https://doi.org/10.1016/j.phrs.2012.10.006>
85. Mattei D, Ivanov A, Ferrai C et al (2017) Maternal immune activation results in complex microglial transcriptome signature in the adult offspring that is reversed by minocycline treatment. *Transl Psychiatry* 7:e1120. <https://doi.org/10.1038/tp.2017.80>
86. Rooney S, Sah A, Unger MS et al (2020) Neuroinflammatory alterations in trait anxiety: modulatory effects of minocycline. *Transl Psychiatry* 10:256. <https://doi.org/10.1038/s41398-020-00942-y>
87. Wang J, Lai S, Li G et al (2020) Microglial activation contributes to depressive-like behavior in dopamine D3 receptor knockout mice. *Brain Behav Immun* 83:226–238. <https://doi.org/10.1016/j.bbi.2019.10.016>
88. Sellgren CM, Gracias J, Watmuff B et al (2019) Increased synapse elimination by microglia in schizophrenia patient-derived models of synaptic pruning. *Nat Neurosci* 22:374–385. <https://doi.org/10.1038/s41593-018-0334-7>
89. Kumar V, Singh BK, Chauhan AK et al (2016) Minocycline rescues from zinc-induced nigrostriatal dopaminergic neurodegeneration: biochemical and molecular interventions. *Mol Neurobiol* 53:2761–2777. <https://doi.org/10.1007/s12035-015-9137-y>
90. Hashimoto K, Tsukada H, Nishiyama S et al (2007) Protective effects of minocycline on the reduction of dopamine transporters in the striatum after administration of methamphetamine: a positron emission tomography study in conscious monkeys. *Biol Psychiatry* 61:577–581. <https://doi.org/10.1016/j.biopsych.2006.03.019>
91. Bierhaus A, Wolf J, Andrassy M et al (2003) A mechanism converting psychosocial stress into mononuclear cell activation. *Proc Natl Acad Sci U S A* 100:1920–1925. <https://doi.org/10.1073/pnas.0438019100>
92. Salvador AF, de Lima KA, Kipnis J (2021) Neuromodulation by the immune system: a focus on cytokines. *Nat Rev Immunol* 21:526–541. <https://doi.org/10.1038/s41577-021-00508-z>
93. Cabib S, Puglisi-Allegra S (2012) The mesoaccumbens dopamine in coping with stress. *Neurosci Biobehav Rev* 36:79–89. <https://doi.org/10.1016/j.neubiorev.2011.04.012>
94. Lieberman OJ, McGuirt AF, Mosharov EV et al (2018) Dopamine triggers the maturation of striatal spiny projection neuron excitability during a critical period. *Neuron* 99:540–554.e4. <https://doi.org/10.1016/j.neuron.2018.06.044>
95. Areal LB, Blakely RD (2020) Neurobehavioral changes arising from early life dopamine signaling perturbations. *Neurochem Int* 137:104747. <https://doi.org/10.1016/j.neuint.2020.104747>
96. Park AT, Tooley UA, Leonard JA et al (2021) Early childhood stress is associated with blunted development of ventral tegmental area functional connectivity. *Dev Cogn Neurosci* 47:100909. <https://doi.org/10.1016/j.dcn.2020.100909>
97. Treadway MT, Cooper JA, Miller AH (2019) Can't or won't? Immunometabolic constraints on dopaminergic drive. *Trends Cogn Sci* 23:435–448. <https://doi.org/10.1016/j.tics.2019.03.003>
98. Felger JC, Miller AH (2012) Cytokine effects on the basal ganglia and dopamine function: the subcortical source of inflammatory malaise. *Front Neuroendocrinol* 33:315–327. <https://doi.org/10.1016/j.yfrne.2012.09.003>
99. Tanaka K, Furuyashiki T, Kitaoka S et al (2012) Prostaglandin E2-mediated attenuation of mesocortical dopaminergic pathway is critical for susceptibility to repeated social defeat stress in mice. *J Neurosci* 32:4319–4329. <https://doi.org/10.1523/JNEUROSCI.5952-11.2012>
100. Vancassel S, Capuron L, Castanon N (2018) Brain kynurenine and BH4 pathways: relevance to the pathophysiology and treatment of inflammation-driven depressive symptoms. *Front Neurosci* 12:499. <https://doi.org/10.3389/fnins.2018.00499>
101. Stanton CH, Holmes AJ, Chang SWC, Joormann J (2019) From stress to anhedonia: molecular processes through functional circuits. *Trends Neurosci* 42:23–42. <https://doi.org/10.1016/j.tins.2018.09.008>
102. Thöny B, Auerbach G, Blau N (2000) Tetrahydrobiopterin biosynthesis, regeneration and functions. *Biochem J* 347(Pt 1):1–16
103. Ng J, Papandreou A, Heales SJ, Kurian MA (2015) Monoamine neurotransmitter disorders—clinical advances and future perspectives. *Nat Rev Neurol* 11:567–584. <https://doi.org/10.1038/nrneuro.2015.172>
104. Zelikowsky M, Hui M, Karigo T et al (2018) The neuropeptide Tac2 controls a distributed brain state induced by chronic social isolation stress. *Cell* 173:1265–1279.e19. <https://doi.org/10.1016/j.cell.2018.03.037>
105. Al Abed AS, Reynolds NJ, Dehorter N (2021) A second wave for the neurokinin Tac2 pathway in brain research. *Biol Psychiatry* 90:156–164. <https://doi.org/10.1016/j.biopsych.2021.02.016>
106. Paul EJ, Tossell K, Ungless MA (2019) Transcriptional profiling aligned with in situ expression image analysis reveals mosaically expressed molecular markers for GABA neuron sub-groups in the ventral tegmental area. *Eur J Neurosci* 50:3732–3749. <https://doi.org/10.1111/ejn.14534>
107. Cadet JL, McCoy MT, Cai NS et al (2009) Methamphetamine preconditioning alters midbrain transcriptional responses to methamphetamine-induced injury in the rat striatum. *PLoS ONE* 4:e7812. <https://doi.org/10.1371/journal.pone.0007812>
108. Batista G, Hensch TK (2019) Critical period regulation by thyroid hormones: potential mechanisms and sex-specific aspects. *Front Mol Neurosci* 12:77. <https://doi.org/10.3389/fnmol.2019.00077>
109. Chatzitomaris A, Hoermann R, Midgley JE et al (2017) Thyroid allostasis-adaptive responses of thyrotropic feedback control to conditions of strain, stress, and developmental programming. *Front Endocrinol (Lausanne)* 8:163. <https://doi.org/10.3389/fendo.2017.00163>
110. Merlino DJ, Barton JR, Charsar BA et al (2019) Two distinct GUCY2C circuits with PMV (hypothalamic) and SN/VTA (mid-brain) origin. *Brain Struct Funct* 224:2983–2999. <https://doi.org/10.1007/s00429-019-01949-y>
111. Yazir Y, Utkan T, Aricioglu F (2012) Inhibition of neuronal nitric oxide synthase and soluble guanylate cyclase prevents depression-like behaviour in rats exposed to chronic unpredictable mild stress. *Basic Clin Pharmacol Toxicol* 111:154–160. <https://doi.org/10.1111/j.1742-7843.2012.00877.x>
112. Ebisutani N, Fukui H, Nishimura H et al (2020) Decreased colonic guanylin/uroguanylin expression and dried stool property in mice with social defeat stress. *Front Physiol* 11:599582. <https://doi.org/10.3389/fphys.2020.599582>
113. Picciotto MR, Brabant C, Einstein EB et al (2010) Effects of galanin on monoaminergic systems and HPA axis: potential mechanisms underlying the effects of galanin on addiction- and stress-related behaviors. *Brain Res* 1314:206–218. <https://doi.org/10.1016/j.brainres.2009.08.033>
114. Han W, Tellez LA, Perkins MH et al (2018) A neural circuit for gut-induced reward. *Cell* 175:887–888. <https://doi.org/10.1016/j.cell.2018.10.018>
115. Jena A, Montoya CA, Mullaney JA et al (2020) Gut-brain axis in the early postnatal years of life: a developmental perspective. *Front Integr Neurosci* 14:44. <https://doi.org/10.3389/fnint.2020.00044>
116. García-Cabrero R, Carbia C, Riordan KJO et al (2021) Microbiota-gut-brain axis as a regulator of reward processes. *J Neurochem* 157:1495–1524. <https://doi.org/10.1111/jnc.15284>
117. Ferré S (2017) Hormones and neuropeptide receptor heteromers in the ventral tegmental area. Targets for the treatment of loss of control of food intake and substance use disorders. *Curr*

Treat Options Psychiatry 4:167–183. <https://doi.org/10.1007/s40501-017-0109-x>

118. Wolf SA, Boddeke HWGM, Kettenmann H (2017) Microglia in physiology and disease. *Annu Rev Physiol* 79:619–643. <https://doi.org/10.1146/annurev-physiol-022516-034406>

Publisher's Note Springer Nature remains neutral with regard to jurisdictional claims in published maps and institutional affiliations.